

TITLE: Systolic Diastolic Partial Volume Differences on ECG-Gated Rb-82 Cardiac PET for Partial Volume Correction of Absolute Myocardial Uptake

AUTHORS AND AFFILIATIONS:

1. Nils P. Johnson, M.D.¹
2. K. Lance Gould, M.D.²

1. Division of Cardiology, Department of Medicine, Northwestern University Feinberg School of Medicine, Chicago, Illinois

2. Weatherhead P.E.T. Center For Preventing and Reversing Atherosclerosis, Division of Cardiology, Department of Medicine, University of Texas Medical School and Memorial Hermann Hospital, Houston, Texas

DISCLAIMERS: None.

CORRESPONDENCE AND REQUESTS FOR REPRINTS:

K. Lance Gould, M.D.,

University of Texas Medical School, 6431 Fannin St., Room 4.256 MSB, Houston, TX 77030

Phone: 713-500-6611, Fax: 713-500-6615, Email: K.Lance.Gould@uth.tmc.edu

FIRST AUTHOR CONTACT INFORMATION:

Nils P Johnson MD (cardiology fellow),

Division of Cardiology, Northwestern University, 676 N. St. Clair, Suite 600, Chicago, IL 60611

Phone: 312-695-1105, Fax: 312-695-1434, Email: n-johnson4@md.northwestern.edu

COUNTS: 5,779 words in document

BRIEF TITLE: Partial Volume Correction for Cardiac PET

ABSTRACT

Systolic images of gated cardiac PET have visually greater myocardial intensity and quantitative count recovery than diastolic images due to greater partial volume loss caused by thinner diastolic LV wall thickness versus systole. Since systolic LV wall thickness is large enough for accurate quantification without partial volume correction, the diastolic/systolic activity ratio measures the partial volume loss on diastolic relative to systolic images or inversely, the systolic/diastolic activity ratio corrected for heart rate is the partial volume correction for quantitative perfusion PET.

Methods: Patients underwent diagnostic myocardial perfusion rest-dipyridamole PET using Rb-82 with and without 8 bin ECG-gating. Decay corrected absolute activity in $\mu\text{Ci}/\text{cc}$ was determined by calibrated linear conversion confirmed by quantitative phantom studies for diastolic, systolic, and combined whole cycle images. Whole-cycle partial volume correction was determined for different heart rates contributing different proportional systolic-diastolic activity to whole cycle perfusion images and compared with partial volume loss for “hot spot” and “cold spot” phantoms of known activity and dimensions.

Results: A total of 264 cardiac PET images were acquired from 159 patient comprised of 105 paired (rest and stress) images and 54 individual (rest or stress) images. The average partial volume correction was 1.14 ± 0.04 . The partial volume corrections with and without accounting for individual heart rates for each image were identical. Partial volume corrections during rest (1.14 ± 0.03) and stress (1.16 ± 0.04) were clinically comparable, within 2% of each other. Partial volume correction for phantom dimensions similar to LV wall thickness was comparable to systolic/diastolic ratios.

Conclusion: Cardiac positron emission tomography (PET) measures absolute myocardial perfusion in $\text{cc}/\text{min}/\text{gm}$ that requires partial volume corrections, herein determined clinically from the systolic/diastolic absolute activity ratio for rest and stress conditions and range of heart rates with dipyridamole stress.

KEY WORDS

1. PET-CT imaging

2. partial volume correction

3. myocardial perfusion

INTRODUCTION

Measuring absolute myocardial perfusion in cc/min/gm at rest and stress, with absolute coronary flow reserve, is important for quantifying the severity of coronary artery disease as a guide to management (1-2). Percent narrowing of focal stenosis is inadequate for assessing severity or functional significance as a guide to invasive procedures (3) given the possible superposition of diffuse coronary atherosclerosis (4), multiple stenoses (5), variable heterogeneous remodeling (2) and heterogeneous endothelial dysfunction. Because of these anatomic complexities, there is only a weak correlation between percent stenosis, coronary flow reserve, fractional flow reserve or absolute maximal perfusion in cc/min/gm in clinical studies (6-7).

Cardiac positron emission tomography (PET) offers a robust, noninvasive measurement of absolute myocardial perfusion in cc/min/gm (8). However, quantitative cardiac PET requires correction for partial volume loss associated with its borderline reconstructed resolution for left ventricular (LV) wall thickness of less than 1.0 to 1.5 cm (9). While the sample voxel size is reportedly a few millimeters for PET-CT scanners, the resolution of reconstructed clinical images is substantially worse due to many factors. The adverse factors degrading resolution include the intrinsic positron range of the tracer, reconstruction noise, poor count density, background activity, "cold spot" versus "hot spot" imaging (10) and blurring, smearing or "dilution" of activity over the space of LV wall motion caused by contraction or translation or respiratory-induced movement of the LV wall in the sample space of the scanner.

Consequently, systolic images of gated cardiac PET have visually greater myocardial intensity and quantitative myocardial count density than diastolic images, as shown schematically in Figure 1. Quantitative myocardial activity in $\mu\text{Ci/cc}$ of systolic images is correspondingly higher than diastolic images despite identical myocardial activity, identical scaling, identical normalization for duration of acquisition to one second, and a fixed number of ECG-gated bins for all heart rates. Lower diastolic count recovery compared to systole can produce artifactual inhomogeneity on ungated studies in normal subjects (11).

The difference between systolic and diastolic quantitative recovery of absolute myocardial activity using ECG-gated cardiac PET arises from the greater partial volume loss caused by the thinner diastolic LV wall thickness compared to systolic LV wall thickness. The normal systolic LV wall thickness is

theoretically large enough on average for accurate count rate quantification without partial volume correction. Therefore, the ratio of diastolic to systolic myocardial activity on ECG-gated PET images measures the partial volume loss on diastolic images relative to systolic images for an individual patient. The inverse, or systolic/diastolic activity ratio, is the corresponding partial volume correction if the different proportional contribution of systolic-diastolic activity to whole cycle (i.e., “ungated”) perfusion images is accounted for.

Given the clinical need for accurate recovery of absolute myocardial activity using cardiac PET, we propose and validate a theoretical and clinical framework for determining the partial volume correction for a given scanner.

MATERIALS AND METHODS

Study Patients

We studied patients undergoing diagnostic myocardial perfusion rest-dipyridamole PET for potential coronary artery disease (CAD) or follow-up imaging at the Weatherhead PET Center for Preventing and Reversing Atherosclerosis of the University of Texas Medical School-Houston and Memorial Hermann Hospital. All subjects signed a clinical informed consent approved by the Committee for the Protection of Human Subjects of the University of Texas Health Science Center.

PET Acquisition Protocol

Patients were instructed to fast for 4 hours and abstain from caffeine, theophylline, and cigarettes for 24 hours before the study. Cardiac PET was performed using a Discovery ST 16-slice PET-computed tomography (CT) multislice bismuth germanate tomograph (GE Healthcare) in two-dimensional mode with extended septa at a reconstructed inplane resolution of 5.9 mm full width at half maximum (FWHM) (12). Patients were positioned in the scanner using laser guides aligned to the base of the throat and confirmed by a CT scout scan. External body markers were used to ensure correct positioning throughout data acquisition. Emission images were obtained over 6 minutes after intravenous injection of 1,295–1,850

MBq (35–50 mCi) of generator-produced Rb-82 and contained 24–60 million total counts, of which 12–30 million were true coincidence counts.

Immediately after completing the resting Rb-82 scan, dipyridamole (0.142 mg/kg/min) was infused for 4 minutes. Four minutes after completion of the dipyridamole infusion, the same dose of Rb-82 was given intravenously. Emission image acquisition was started at 70 seconds (or 80 seconds for patients with heart failure or heart rates below 55 beats per minute) after the beginning of Rb-82 infusion. For dipyridamole-induced angina, aminophylline (125 mg) was given intravenously.

Three surface ECG leads on the patient were placed to ensure a large magnitude and reliable QRS complex for ECG-gating. True coincidence counts were divided into 8 equally-sized temporal R-R bins. All protocols, data acquisition, processing and quantification of cardiac PET are as previously reported (13-17).

CT scans for attenuation correction were acquired before rest emission imaging and after stress emission imaging. Protocols for CT acquisition and for ensuring alignment between PET emission and CT attenuation are as previously reported (18-19).

Image Reconstruction

Custom software allowed shifting of the CT data to align the heart borders visually with the PET data to achieve good co-registration. Images were reconstructed using filtered backprojection with a Butterworth filter having a cutoff of 0.55, roll-off of 10, and pixel size of 3.27 X 3.27 mm.

After attenuation correction, the reconstructed PET emission images in DICOM format with quantitative header data were exported to an Ultra 60 workstation (Sun Microsystems) of an mPower-HZL PET scanner (Positron Corporation) for reorientation into long- and short-axis tomographic and topographic three-dimensional displays using previously described automated quantitative software (13-17).

A three-dimensional restructuring algorithm generates true short- and long-axis views from reconstructed PET transaxial cardiac images, perpendicular and parallel to the long axis of the left ventricle. From the tomographic data, circumferential profiles of each short axis slice are used to reconstruct three-dimensional topographic views of the entire LV and lateral, inferior, septal, and anterior

quadrant views of the three-dimensional topographic display corresponding to coronary artery distributions as previously described (13-17). The basal four slices were not used for quantitative analysis due to the low counts in the membranous inter-ventricular septum. The apical two slices were not used for quantitative analysis due to potential partial volume errors caused by partial thickness slices through the tip of the LV.

Quantitative PET Image Analysis

Absolute activity recovered by the scanner was computed by converting the raw counts to activity in $\mu\text{Ci/cc}$ using a linear calibrated conversion formula in automated software after quantitative GE-to-Positron conversion had been validated by phantom experiments. Of the 8 ECG-gated R-R bins, the bins 3 and/or 4 after the start of the QRS complex peak were taken as systole and the remaining bins 1, 2, 4 or 5 through 8 were taken as diastole based on those bin images best bracketing systole visually for each case. In some instances, bin 3 or 4 alone bracketed systole completely. Images representing diastole, systole, and both diastole and systole added together were decay corrected and normalized to absolute activity in $\mu\text{Ci/cc}$ in one second. An image representing the ratio of systolic to diastolic activity was also created.

Ejection fraction was computed by the semi-automated, endocardial-epicardial border tracking algorithm of the Emory Toolbox program (20) that is an option in the GE scanner operating system. The LV diastolic dimension was computed using a mid-cavity slice from the circumferential profiles used to reconstruct three-dimensional topographic views of the ventricle during the diastolic bins.

Clinical Data and Duration of Systole

Height and weight were measured on the day of PET imaging. Body-mass index in units of kg/m^2 was computed as the weight divided by the square of the height. Heart rate was determined from the 12-lead stress test ECG monitor and recorded log at the beginning of image acquisition and was constant throughout the short image acquisition time for Rb-82. An additional 3-lead monitor was used for ECG gating of the PET images that recorded the same heart rate.

The reported relationship between heart rate and the proportion of the R-R interval spent in systole (21) used the following formulae:

$$\text{systolic fraction of R-R interval} = RR_{\text{sys}} = 0.01 \cdot \exp(4.14 - 40.74/\text{heart rate}), \quad (\text{Equ. 1})$$

$$\text{diastolic fraction of R-R interval} = RR_{\text{dia}} = 1 - RR_{\text{sys}}, \quad (\text{Equ. 2})$$

where heart rate is in beats per minute (bpm). Alternatively, the more simplistic assumption that 1/3 of the R-R interval represents systole ($RR_{\text{sys}}=1/3$) and 2/3 of the R-R interval represents diastole ($RR_{\text{dia}}=2/3$), independent of heart rate, was also examined.

Partial Volume Correction

The principle used for determining the partial volume correction is illustrated in the schematic of Figure 1. The thinner diastolic LV wall causes partial volume loss of activity recovered by the scanner as compared to the thicker systolic wall for which activity recovery by the scanner is correct without a partial volume error. This figure also shows the spreading function of limited resolution wherein the wall thickness on the image is thicker than it actually is in-vivo. If cardiac PET images had no partial volume loss (partial volume correction = 1.0), diastolic and systolic myocardial absolute activity in $\mu\text{Ci/cc}$ would be identical for various systolic and diastolic intervals of the heart contraction cycle.

The total partial volume correction for the combined systolic and diastolic image (i.e. “ungated” images) depends on the partial volume correction (or partial volume loss) for diastole (D_{pvc}), on the partial volume correction for systole (S_{pvc}), and on the relative proportion or fraction of the R-R interval spent in systole (RR_{sys}) and diastole (RR_{dia}). The total partial volume correction (T_{pvc}) is therefore given by the following equation:

$$T_{\text{pvc}} = RR_{\text{sys}} \times S_{\text{pvc}} + RR_{\text{dia}} \times D_{\text{pvc}}. \quad (\text{Equ. 3})$$

As will be shown in the results section, our phantom data demonstrate that $S_{\text{pvc}} \approx 1.0$. Thus, the diastolic partial volume correction is then given by the systolic/diastolic ratio of absolute activity ($AA_{\text{s/d}}$). The total partial volume correction equation then becomes:

$$T_{\text{pvc}} = RR_{\text{sys}} + (1 - RR_{\text{sys}}) \times AA_{\text{s/d}}. \quad (\text{Equ. 4})$$

Phantom Studies

As a separate, independent, traditional check on our in-vivo imaging data, both “hot spot” and “cold spot” phantoms were imaged for accuracy of quantitative recovery of activity by the PET-CT scanner. Image reconstruction parameters were identical to those used for patient studies. For “hot spot” imaging, a tree-like phantom (the Mullani “finger” phantom) with angled branches of varying width (22) was scanned after being filled by a uniform 12.7 $\mu\text{Ci/cc}$ concentration of F-18 activity. PET-CT imaging was done over 5 minutes acquiring 102.7M counts with CT attenuation correction and automated decay correction by scanner software for comparison to activity measured in a calibrated well counter with manually calculated decay correction of the known starting concentration in the phantom. Figure 2 shows the shape and dimensions of the phantom, and a representative image of its relative activity. The recovered activity in regions with 1.5 cm and 1.0 cm diameter, corresponding to approximate systolic and diastolic LV thickness (23-24), was determined by converting the raw counts to activity in $\mu\text{Ci/cc}$ using the GE commercial calibration confirmed by a linear calibrated conversion formula validated by additional prior phantom experiments. This imaged activity recovery was compared to the known activity concentration in the phantom based on precise well counter measurements decay corrected for the time of filling and imaging the phantom.

The ratio of recovered activity to true activity gives the partial volume loss and its inverse is the partial volume correction factor. For the larger sections of the phantom, 1.5 cm or greater, the quantitative activity imaged by the PET-CT and automatically quantified by the Positron quantitative software and calibration factors equals the known activity concentration in the phantom as determined by a well counter calibrated against known standard activity.

F-18 was chosen as the phantom tracer given that its positron range in tissue is smaller than that for the common perfusion tracer Rb-82. As such, it introduces less “blur” into phantom boundaries than if Rb-82 had been chosen. Therefore if complete count recovery occurs in the regions with 1.5 cm diameter with F-18, then complete count recovery would occur in these regions if Rb-82 were used instead.

For testing the quantitative recovery of activity for “cold spot” imaging, a Delux Jasaczac Phantom (25) consisting of solid plastic spheres in a 22 cm diameter cylinder was filled with 3.83 $\mu\text{Ci/cc}$ of F-18 and imaged for 20 minutes, acquiring 160M counts. Figure 3 shows the solid spheres of varying diameter that produce negative “cold spot” defects for testing quantitative recovery of activity in perfusion defects.

The spillover of activity into the smallest “cold spot” defect is due to the partial volume error and spreading function of limited resolution as illustrated in Figure 1, also called “spillover”.

Statistical Methods

All statistical tests were performed using STATA version 10.1 (StataCorp, College Station, Texas). Continuous variables are expressed as mean \pm standard deviation and were compared using the t-test. Paired data was compared using a paired t-test. All applicable tests were two-tailed, and a $p < 0.05$ was taken as the cutoff for statistical significance.

RESULTS

Figure 4 illustrates tomographic views of relative myocardial activity in diastole and systole scaled to the maximum activity of the entire data set of the PET-CT scanner. The systolic images have 18% more activity than diastolic images in this example when systolic and diastolic images are normalized or scaled to the same maximum activity. Although the myocardial activity is the same in diastole and systole, the diastolic images appear to have less activity than the systolic activity due to the greater partial volume loss caused by the thinner LV wall during diastole. Figure 5 shows this same data set converted to absolute activity in $\mu\text{Ci/cc}$ where diastole and systole are normalized to their own maximum that is scaled to the separate maximum $\mu\text{Ci/cc}$ of diastole and systole by the Positron automated quantitative software. Since the diastolic and systolic images are scaled to their own maximum, the images look similar but the absolute quantitative scale defines the quantitative differences.

A total of 159 patient studies produced 105 paired (rest and stress) images and 54 individual (rest or stress) images for a total of 264 PET acquisitions. All patients were free of atrial fibrillation during image acquisition, and the vast majority had a normal ($\geq 55\%$) ejection fraction (220 of 264 acquisitions). Only 4 studies had an ejection fraction $< 40\%$, and no study had one $< 34\%$. Patients were selected over the entire spectrum of coronary artery disease, from normal screening, to those with known myocardial infarction, to second opinions, or to those going for bypass surgery.

Table 1 shows clinical and imaging parameters for all acquisitions. Activity recovery in systole is higher (1.90 $\mu\text{Ci/cc}$) compared to diastole (1.57 $\mu\text{Ci/cc}$), $p < 0.0001$ for a difference of $0.32 \pm 0.13 \mu\text{Ci/cc}$. The average partial volume correction factor is 1.14 for assumed 1/3 systolic and 2/3 diastolic fractions of the RR interval regardless of heart rate. Alternatively, the average partial volume correction adjusted for systolic-diastolic fractions at the different heart rates for each image is also 1.14 with a slight statistical difference (difference= $0.004 \pm 0.0.12$, $p < 0.0001$). Therefore, the partial volume corrections with and without accounting for individual heart rates for each image are identical for clinical purposes.

Partial Volume Correction Over A Wide Range Of Heart Rates

Table 2 computes the theoretical partial volume correction over a wide range of heart rates using the average systolic/diastolic activity ratio from Table 1. As can be seen, the partial volume correction remains nearly identical regardless of the heart rate even at the extremes of 45 and 100 beats per minute that show 1.8% ($[1.16-1.14]/1.16$) over or under the partial volume correction at an intermediate heart rate of 71. Therefore, it is not necessary to adjust the systolic-diastolic partial volume correction for individual heart rate in each image.

Paired Images

Table 3 shows clinical and imaging parameters for all 105 paired (rest and stress) acquisitions. While statistically different, the partial volume corrections for rest (1.14 ± 0.03) and stress (1.16 ± 0.04) are clinically comparable, within 2% of each other.

Phantom Data for Partial Volume Correction

Table 4 gives the recovered activity in the finger phantom for dimensions similar to those observed during LV systole and diastole. The partial volume correction for systolic dimensions is near unity ($S_{pvc} \approx 1.0$). Using the phantom derived ratio of absolute activity between systole and diastole ($AA_{s/d}$), the total partial volume correction for a heart rate of 71 bpm (with $RR_{sys}=0.35$ and $RR_{dia}=0.65$ via

equations (1-2) above) can be derived as follows: estimated phantom total partial volume correction = $T_{pvc} = (0.35)(1.002) + (0.65)(1.279) = 1.18$, that approximates the average clinically observed $AA_{s/d}=1.21$ from the human data in Table 1. The partial volume correction from the phantom data does not account for the additional in-vivo variables that the systolic/diastolic ratio incorporates. The phantom-based partial volume correction would therefore be expected to be slightly lower than the in-vivo partial volume correction uncorrected for heart rate.

The quantitative activity recovery in the center of each finger of Figure 2 is identical for the 1.5 and 3 cm thicknesses. The minimal visual variability is not quantitatively significant as measured at the center of each finger, just as the activity in the LV wall was automatically measure at the peak of the radial units of the rotated cross-sectional images. The mild visual variability is due to two factors: (i) at the edges of the phantom finger, partial volume losses do occur interacting with reconstruction and background noise to make the edges “moth-eaten” in appearance; (ii) we use color scaling to enhance contrast or density variation that would not be apparent in black and white.

Reconstruction at best resolution of the of the PET-CT for cold spot defects of the Jasaczac Phantom in Figure 3 shows that a perfusion defect of approximately 12.7 mm is the smallest defect for accurate quantification of low activity in the perfusion defect. We have also previously demonstrated contrast resolution is superior with filtered back projected reconstruction compared to ordered subset expectation maximization (OSEM) reconstruction for quantifying “cold spot” images (10).

DISCUSSION

Quantification of myocardial perfusion by PET in cc/min/gm and absolute coronary flow reserve (8) is important for defining severity of both diffuse and segmental coronary artery disease (2). However, for accurate quantitative measurements, partial volume loss must be corrected due to limited reconstructed resolution for left ventricular (LV) wall thickness of less than 1.0 to 1.5 cm (9).

Our results support several conclusions. First, partial volume corrections with and without accounting for individual heart rates for each image are identical for clinical purposes. Second, partial volume corrections for rest and stress are clinically comparable. Third, this validated framework can be applied to any scanner to define its partial volume correction factors empirically. Taken together, these

findings enable the robust recovery of absolute myocardial activity necessary for quantitative perfusion (8).

Comparison to Existing Literature

Several alternative methods have been used to account for partial volume effects in cardiac PET imaging. Some have utilized anatomic information from other imaging modalities, such as echocardiography, magnetic resonance imaging, or CT to develop geometric models for partial volume correction (9). Dual modality PET-CT scanners may be more suited to this task than historical stand-alone PET scanners that make image fusion between modalities more laborious. Others have added parameters into quantitative flow models to account for partial volume effects (26). However, these approaches require questionable assumptions, add complexity and potential numerical instability to the modeling and require dynamic imaging (27) which reduces counts in each image and reduces signal-to-noise compared to integrative models (8). Some work has been done using sinogram region of interest analysis (27). A few reports exist of imaging only patients with LV hypertrophy from hypertrophic cardiomyopathy in an attempt to minimize partial volume effects (28).

The reported sample voxel size of 3.25x3.25x3.25 mm for the PET-CT scanner does not account for or reflect degradation of resolution by reconstruction noise, poor count density, background activity, and differences between in-plane versus z-axis resolution. Consequently, theoretical partial volume corrections are open to question since they do not account for these in-vivo clinical variations affecting effective clinical resolution and associated accuracy of quantitative activity recovery by the scanner. However, our in-vivo clinical method here reported by definition accounts for these variables as a robust partial volume correction for clinical application that, as expected, are somewhat larger than partial volume corrections based on in-vitro phantom studies.

Limitations of the Study

The partial volume correction based on the systolic/diastolic activity ratio is applicable to different patients and different heart sizes over a wide range of heart rates during rest-dipyridamole PET perfusion

imaging as well as a range of ejection fractions. However, for thin-walled regions of the left ventricle with little systolic wall thickening, the average partial volume correction that is usually applicable to most hearts will underestimate the partial volume correction needed. This underestimation is due to the LV wall thickness remaining less than scanner resolution throughout the RR interval as compared to the normal heart wherein wall thickness approximates scanner resolution with full activity recovery for approximately one third of the RR interval. For such thin, non-thickening regions of the LV wall, the partial volume correction is better approximated by the systolic/diastolic ratio 1.21 that is not weighted downward to lower values by the adjustment for systole one-third and diastolic two-thirds of the RR interval.

These corrections for partial volume loss of scanner activity recovery do not correct for the spillover of activity into a negative perfusion defect. However, as shown in Figure 3, scanner resolution is adequate for quantifying activity of a negative perfusion defect of 12.7 mm or greater in diameter, adequate for clinical purposes.

The above technique relies on the approximation that scanner resolution is sufficient to avoid partial volume correction during systole. For older generation scanners, this approximation may not hold and would underestimate the partial volume coefficient.

CONCLUSIONS

Partial volume correction is necessary in cardiac PET to recover absolute myocardial activity accurately. This study demonstrates robust partial volume correction for quantitative cardiac PET scanning from the systolic/diastolic ratio of absolute activity of ECG-gated studies for both rest and stress conditions over the range of observed heart rates during dipyridamole stress consistent with activity recovery from phantoms of size and activity comparable to LV wall thickness.

REFERENCES

1. Gould KL. Positron emission tomography in coronary artery disease. *Curr Open Cardio*. 2007;22:422-428.
2. Gould KL. Does coronary flow trump coronary anatomy? *JACC Cardiovasc Imaging*. 2009;2:1009-1023.
3. Topol EJ, Nissen SE. Our preoccupation with coronary luminology. The dissociation between clinical and angiographic findings in ischemic heart disease. *Circulation*. 1995;92:2333-2342.
4. De Bruyne B, Hersbach F, Pijls NH, et al. Abnormal epicardial coronary resistance in patients with diffuse atherosclerosis but "Normal" coronary angiography. *Circulation*. 2001;104:2401-2406.
5. De Bruyne B, Pijls NH, Heyndrickx GR, Hodeige D, Kirkeeide R, Gould KL. Pressure-derived fractional flow reserve to assess serial epicardial stenoses: theoretical basis and animal validation. *Circulation*. 2000;101:1840-1847.
6. White CW, Wright CB, Doty DB, et al. Does visual interpretation of the coronary arteriogram predict the physiologic importance of a coronary stenosis? *N Engl J Med*. 1984;310:819-824.
7. Meijboom WB, Van Maugham CA, van Pelt N, et al. Comprehensive assessment of coronary artery stenoses: computed tomography coronary angiography versus conventional coronary angiography and correlation with fractional flow reserve in patients with stable angina. *J Am Coll Cardio*. 2008;52:636-643.
8. Yoshida K, Mullani N, Gould KL. Coronary flow and flow reserve by PET simplified for clinical applications using rubidium-82 or nitrogen-13-ammonia. *J Nucl Med*. 1996;37:1701-1712.

9. Porenta G, Kuhle W, Sinha S, et al. Parameter estimation of cardiac geometry by ECG-gated PET imaging: validation using magnetic resonance imaging and echocardiography. *J Nucl Med.* 1995;36:1123-1129.
10. Wollenweber SD, Gould KL. Investigation of cold contrast recovery as a function of acquisition and reconstruction parameters for 2D cardiac PET. *IEEE Nuclear Science Symposium Conference Record* 2005;5:2552-2556.
11. Bartlett ML, Bacharach SL, Voipio-Pulkki LM, Dilsizian V. Artifactual inhomogeneities in myocardial PET and SPECT scans in normal subjects. *J Nucl Med.* 1995;36:188-195.
12. Teräs M, Tolvanen T, Johansson JJ, Williams JJ, Knuuti J. Performance of the new generation of whole-body PET/CT scanners: Discovery STE and Discovery VCT. *Eur J Nucl Med Mol Imaging.* 2007;34:1683-1192.
13. Bartlett ML, Bacharach SL, Voipio-Pulkki LM, Dilsizian V. Artifactual inhomogeneities in myocardial PET and SPECT scans in normal subjects. *J Nucl Med.* 1995;36:188-195.
14. Gould KL, Ornish D, Scherwitz L, et al. Changes in myocardial perfusion abnormalities by positron emission tomography after long-term, intense risk factor modification. *JAMA.* 1995;274:894-901.
15. Gould KL, Martucci JP, Goldberg DI, et al. Short-term cholesterol lowering decreases size and severity of perfusion abnormalities by positron emission tomography after dipyridamole in patients with coronary artery disease. A potential noninvasive marker of healing coronary endothelium. *Circulation.* 1994;89:1530-1538.
16. Sdringola S, Nakagawa K, Nakagawa Y, et al. Combined intense lifestyle and pharmacologic lipid treatment further reduce coronary events and myocardial perfusion abnormalities compared with usual-care cholesterol-lowering drugs in coronary artery disease. *J Am Coll Cardio.* 2003;41:263-272.

17. Gould KL. Assessing progression or regression of CAD: the role of perfusion imaging. *J Nucl Cardio.* 2005;12:625-638.
18. Sdringola S, Loghin C, Boccalandro F, Gould KL. Mechanisms of progression and regression of coronary artery disease by PET related to treatment intensity and clinical events at long-term follow-up. *J Nucl Med.* 2006;47:59-67.
19. Gould KL, Pan T, Login C, Johnson NP, Guha A, Sdringola S. Frequent diagnostic errors in cardiac PET/CT due to misregistration of CT attenuation and emission PET images: a definitive analysis of causes, consequences, and corrections. *J Nucl Med.* 2007;48:1112-1121.
20. Gould KL, Pan T, Login C, Johnson NP, Sdringola S. Reducing radiation dose in rest-stress cardiac PET/CT by single poststress cine CT for attenuation correction: quantitative validation. *J Nucl Med.* 2008;49:738-745.
21. Hickey KT, Sciacca RR, Bokhara S, et al. Assessment of cardiac wall motion and ejection fraction with gated PET using N-13 ammonia. *Clin Nucl Med.* 2004;29:243-248.
22. Moran D, Epstein Y, Keren G, Laor A, Sherez J, Shapiro Y. Calculation of mean arterial pressure during exercise as a function of heart rate. *Apply Human Sci.* 1995;14:293-295.
23. Mullani NA, Gould KL, Hartz RK, et al. Design and performance of POSICAM 6.5 BGO positron camera. *J Nucl Med.* 1990;31:610-616.
24. Eber LM, Greenberg HM, Cooke JM, Gorlin R. Dynamic changes in left ventricular free wall thickness in the human heart. *Circulation.* 1969;39:455-464.

25. Dodge HT, Frimer M, Stewart DK. Functional evaluation of the hypertrophied heart in man. *Circ Res*. 1974;35:suppl II:122-127.

26. Malawi O, Podoloff DA, Kohl Myer S, et al; National Electrical Manufacturers Association. Performance characteristics of a newly developed PET/CT scanner using NEMA standards in 2D and 3D modes. *J Nucl Med*. 2004;45:1734-1742.

27. Herrero P, Markham J, Bergmann SR. Quantitation of myocardial blood flow with H₂ 15O and positron emission tomography: assessment and error analysis of a mathematical approach. *J Comput Assist Tomogr*. 1989;13:862-873.

28. Muzic RF Jr, Chen CH, Nelson AD. A method to correct for scatter, spillover, and partial volume effects in region of interest analysis in PET. *IEEE Trans Med Imaging*. 1998;17:202-213.

29. Endo M, Yoshida K, Iinuma TA, et al. Noninvasive quantification of regional myocardial blood flow and ammonia extraction fraction using nitrogen-13 ammonia and positron emission tomography. *Ann Nucl Med*. 1987;1:1-6.

TABLES

Table 1. Observed parameters

	Mean \pm SD
Heart rate (bpm)	71 \pm 19
Diastolic whole heart absolute uptake ($\mu\text{Ci/cc}$)	1.57 \pm 0.50
Systolic whole heart absolute uptake ($\mu\text{Ci/cc}$)	1.90 \pm 0.59
Systolic/diastolic activity ratio ($AA_{s/d}$)	1.21 \pm 0.06
Diastolic and systolic whole heart uptake ($\mu\text{Ci/cc}$)	1.60 \pm 0.52
Partial volume correction (systole=1/3 diastole=2/3)*	1.14 \pm 0.04
Partial volume correction (based on heart rate)**	1.14 \pm 0.04
Fraction of R-R spent in systole (RR_{sys})***	0.34 \pm 0.05
Diastolic LV diameter (cm)	5.2 \pm 0.7
Ejection fraction (%)	64.4 \pm 10.4
Weight (lbs)	189.1 \pm 37.1
Body-mass index (kg/m^2)	27.9 \pm 4.9

Note N=264 except for weight and body-mass index which are N=159

* using equation (4) with $RR_{\text{sys}}=1/3$ and $RR_{\text{dia}}=2/3$

** using equation (4) with RR_{sys} from equation (1) and RR_{dia} from equation (2)

*** using equation (1)

bpm = beats per minute

LV = left ventricle

SD = standard deviation

Table 2. Theoretical partial volume corrections by heart rate

Heart rate (bpm)	Systolic fraction*	Diastolic fraction**	Correction equation***	Partial volume correction
45	0.25	0.75	$0.25 + 0.75 \times 1.21$	1.16
59	0.31	0.69	$0.31 + 0.69 \times 1.21$	1.15
71	0.35	0.65	$0.35 + 0.65 \times 1.21$	1.14
87	0.39	0.61	$0.39 + 0.61 \times 1.21$	1.13
100	0.42	0.58	$0.42 + 0.58 \times 1.21$	1.12

* using equation (1)

** using equation (2)

*** using equation (4) and $AA_{s/d}=1.21$ from Table 1

Table 3. Paired rest/stress observations

	Rest	Stress	p
Heart rate (bpm)	59 ± 12	87 ± 17	<0.0001
Diastolic whole heart absolute uptake (μCi/cc)	1.45 ± 0.48	1.56 ± 0.47	<0.0001
Systolic whole heart absolute uptake (μCi/cc)	1.75 ± 0.56	1.94 ± 0.57	<0.0001
Ungated whole heart absolute uptake (μCi/cc)	3.15 ± 0.96	3.93 ± 1.13	<0.0001
Systolic/diastolic activity ratio (AA _{s/d})	1.21 ± 0.04	1.24 ± 0.05	<0.0001
Partial volume correction (systole=1/3 diastole=2/3)*	1.14 ± 0.03	1.16 ± 0.04	<0.0001
Ejection fraction (%)	62.7 ± 8.6	68.5 ± 10.2	<0.0001
Diastolic LV diameter (cm)	5.3 ± 0.6	5.1 ± 0.7	<0.0001

N=105 for all rows

* using equation (4) with $RR_{sys}=1/3$ and $RR_{dia}=2/3$

bpm = beats per minute

LV = left ventricle

Table 4. "Hot spot" finger-like Mullani phantom study of uniform F-18 activity

Diameter	Recovered activity ($\mu\text{Ci/cc}$)	Fraction of actual 12.66 $\mu\text{Ci/cc}$	Partial volume correction
Target 1.5cm (\approx systole)	12.64	0.998	1.002
Target 1cm (\approx diastole)	9.90	0.782	1.279

FIGURE LEGENDS

Figure 1. Schematic representation of short-axis left ventricular activity during diastole (left) and systole (right). Systolic images of gated cardiac PET have greater myocardial intensity and quantitative myocardial count density than diastolic images despite identical scaling, identical normalization for duration of acquisition to one second, and a fixed number of ECG-gated bins for all heart rates. The difference between systolic and diastolic quantitative recovery of absolute myocardial activity using ECG-gated cardiac PET arises from the greater partial volume loss caused by the thinner diastolic LV wall thickness compared to systolic LV wall thickness.

Figure 2. Tree-like phantom (Mullani “finger” phantom (22)) with angled branches of varying width used for “hot spot” imaging. The schematic on the left shows the shape and dimensions of the phantom. The PET-CT image on the right shows its relative activity when filled with a uniform activity. The recovered activity in regions with 1.5 cm and 1.0 cm diameter correspond to approximate systolic and diastolic LV thickness.

Figure 3. Delux Jasaczac Phantom (23) consisting of solid plastic spheres of 9.5, 12.7, 15.9, 19.1, 25.4 and 31.8 mm diameter in a 22 cm diameter cylinder used for “cold spot” imaging. The photo and short-axis schematic on the left show its visual appearance. The PET-CT imaging on the right shows its relative activity when filled with a uniform activity. The spillover of activity into the smallest “cold spot” defect is due to the partial volume error and spreading function of limited resolution as illustrated in Figure 1.

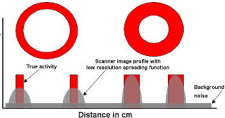
Figure 4. Tomographic views of relative myocardial activity in diastole and systole scaled to the maximum activity of the entire data set of the PET-CT scanner. The systolic images have 18% more activity than diastolic images in this example when systolic and diastolic images are normalized or scaled to the same maximum activity. Although the myocardial activity is the same in diastole and systole, the diastolic images appear to have less activity than the systolic activity due to the greater partial volume loss caused by the thinner LV wall during diastole.

Figure 5. Tomographic views of absolute myocardial activity in kBq/cm^3 from Figure 4, where diastole and systole are normalized to their own maximum that is scaled to the separate maximum kBq/cm^3 of diastole and systole by the Positron automated quantitative software. Since the diastolic and systolic images are scaled to their own maximum, the images look similar but the absolute quantitative scale defines the quantitative differences. Equivalent activities would be $133.2 \text{ kBq}/\text{cm}^3 = 3.6 \text{ } \mu\text{Ci}/\text{cc}$ and $156.9 \text{ kBq}/\text{cm}^3 = 4.24 \text{ } \mu\text{Ci}/\text{cc}$.

Diastole

Systole

Scanner Activity



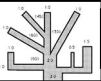
True activity

Scanner image profile with
low resolution spreading function

Background
noise

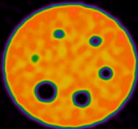
Distance in cm

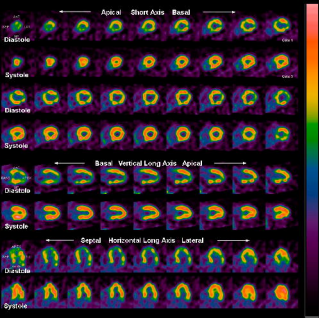
Tree phantom



PET







Diastole



← Superior Horizontal Long Axis Inferior →

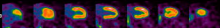
Systole



Diastole
133.2
Systole
158.9

kBq/cm³

Diastole



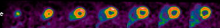
← Basal Vertical Long Axis Apical →

Systole



-1.1

Diastole



← Apical Short Axis Basal →

Systole

